Transworld Research Network
37/661 (2), Fort P.O., Trivandrum-695 023, Kerala, India

Recent Res. Devel. Chem. Physics, 4(2003): 325-344 ISBN: 81-7895-095-2

15 UV, visible and near-IR spectroscopy of atmospheric species

A.C. Vandaele[1], M. De Mazière[1], C. Hermans[1], M. Carleer[2], C. Clerbaux[2] P.F. Coheur[2‡], R. Colin[2], S. Fally[2], B. Coquart[3], A. Jenouvrier[3] and M.-F. Mérienne[3]
[1]Belgian Institute for Space Aeronomy, 3 av. Circulaire, B-1180 Brussels, Belgium
[2]Laboratoire de Chimie Physique Moléculaire, ULB, CP 160/09, 50 av. F.D. Roosevelt, B-1050 Brussels, Belgium; [3]Groupe de Spectrométrie Moléculaire et Atmosphérique, UFR Sciences, BP 1039, F-51687 Reims, Cedex 2, France

Abstract

Spectroscopy in the UV, visible and NIR regions has gained recognition these last decades in atmospheric research through the development of instruments dedicated to the detection of atmospheric species and operating in these spectral regions. Laboratory measurements are needed to deliver high quality reference data. Those can either be line parameters, such as line position, intensity and broadening coefficients, or absorption cross-sections. The use of these reference data in an atmospheric context implies that the laboratory measurements be conducted under temperature and pressure conditions close to the ones prevailing in the atmosphere. As those vary over a large scale, it is necessary to analyse in detail the temperature and pressure dependence of i.e. the absorption cross-sections.

‡Scientific Research Worker with the Fonds National de la Recherche Scientifique

Correspondence/Reprint request: Dr. A. C. Vandaele, Belgian Institute for Space Aeronomy, 3 av. Circulaire, B-1180 Brussels Belgium

UV, VISIBLE AND NEAR-IR SPECTROSCOPY OF ATMOSPHERIC SPECIES

A.C. Vandaele[1], M. De Mazière[1], C. Hermans[1],
M. Carleer[2], C. Clerbaux[2], P.F. Coheur[2‡], R. Colin[2], S. Fally[2],
B. Coquart[3], A. Jenouvrier[3], and M.-F. Mérienne[3]

[1] Belgian Institute for Space Aeronomy, 3 av. Circulaire, B-1180 Brussels, Belgium

[2] Laboratoire de Chimie Physique Moléculaire, ULB, CP 160/09, 50 av. F.D. Roosevelt, B-1050 Brussels, Belgium

[3] Groupe de Spectrométrie Moléculaire et Atmosphérique, UFR Sciences, BP 1039, F-51687 Reims, Cedex 2, France

Running title : UV-VIS-NIR spectroscopy of atmospheric species

‡ Scientific Research Worker with the Fonds National de la Recherche Scientifique

ABSTRACT

Spectroscopy in the UV, visible and NIR regions has gained recognition these last decades in atmospheric research through the development of instruments dedicated to the detection of atmospheric species and operating in these spectral regions. Laboratory measurements are needed to deliver high quality reference data. Those can either be line parameters, such as line position, intensity and broadening coefficients, or absorption cross-sections. The use of these reference data in an atmospheric context implies that the laboratory measurements be conducted under temperature and pressure conditions close to the ones prevailing in the atmosphere. As those vary over a large scale, it is necessary to analyse in detail the temperature and pressure dependence of i.e. the absorption cross-sections. Large variations are observed, which must be taken into account when performing atmospheric soundings.

INTRODUCTION

The climate changes of the last decades have created the need to monitor the changes of the atmospheric composition. The discovery of the ozone hole over Antarctica and of a similar phenomenon in the Arctic, the global warming of the atmosphere through the increasing emissions of man-made greenhouse gases, and the analysis of the effects of volcanic activities on a global scale, are but some examples of issues addressing the political and the public communities.

The complexity of the processes taking place in the Earth's atmosphere requires that a large number of different parameters be measured on a global scale. This is specially the case for the abundances of the trace gases, which can show important spatial variations. The global observation of the trace gases is presently best performed from space-borne instruments, but requires, for validation purposes, simultaneous local measurements from the ground or from balloons to be made. Most of these space- or ground-based measurements use spectroscopic instruments that probe regions of the electromagnetic spectrum extending from the microwave to the UV. The retrieval of abundances from the spectra require validated inversion algorithms, but most importantly strongly depend on the availability of accurate reference spectra or data, which can only be acquired in the laboratory under well-defined and controlled conditions.

The knowledge of the radiative properties of the atmospheric species is also valuable for the modelling of the radiative transfer of the Earth's atmosphere. Of the global average incoming solar radiation at the top of the atmosphere (342 Wm^{-2}) , the Earth's atmosphere reflects about 30% and absorbs 20%, while the surface absorption amounts to 50%. Recent observations [1,2] suggest that the Earth's atmosphere under cloudy-sky conditions might absorb up to 28% of the incoming radiation, i.e. up to 30 Wm^{-2} more than the model predictions. Other studies [3-5] find inexplicable discrepancies of

the order of 40% between models and observations of the clear-sky diffuse field, whereas models do represent the direct normal irradiance within 1%. Several candidates have been proposed for this discrepancy: Clouds [1,2], aerosols [6,7], missing weak H_2O lines [8], errors in the water vapor line intensities [9], H_2O continuum [10], H_2O dimer and other H_2O complexes especially those involving O_2 and N_2 [11,12], or O_2 collision-induced complexes [13,14]. *Zender* [15] estimated the radiative forcing of complexes such as O_2-O_2 and O_2-N_2 and the uncertainties associated therewith. He found that the 20% to 30% uncertainty was essentially due to the uncertainties on the complexes' cross-sections. Laboratory studies are therefore needed to better characterize the absorption of such complexes and that of the H_2O spectrum, which might extend up to the UV.

IR and mid-IR reference data have already been implemented in databases such as HITRAN [16,17] or GEISA [18]. Only recently have such databases been extended to data obtained in the NIR, visible and UV regions. However, many problems remain in these spectral regions and new measurements are needed. Current remote sensing instruments, and in particular laser applications, require for example, that the intensity of well-chosen, isolated, single lines be known to better than 1%. Such high accuracy is not always attained with the existing data. *Newnham* [19] listed the needs in terms of improvement or availability of data for several molecules. Line parameters, including temperature and pressure dependent widths, and intensities, of molecules such as H_2O, O_3, CO or CO_2, should be improved and validated in the NIR region. For many UV-visible absorbing molecules, no high-resolution data are available. Temperature dependent cross-sections are needed and the effect of the pressure broadening has still to be implemented.

Fourier transform (FT) spectrometers have recently superseded conventional grating spectrometers for the measurement of spectroscopic data, even in the UV-visible region. These instruments provide a very high-resolution and wave number-calibrated data. *Newnham* [19] even proposed that Fourier transform spectroscopy should be adopted as the standard technique.

In the following, we will show how the use of FT spectrometry can improve the accuracy of the reference data. The chosen examples cover the spectral range from the NIR to the UV region, and concern the different properties that can be retrieved: Line parameters (positions, intensities, broadening coefficients, pressure shifts) up to the UV region, absorption cross-sections, and collision-induced absorption. Each subject will be illustrated by measurements done by a well-established collaboration between three groups:

- IASB/BIRA (Brussels, Belgium), which is mainly involved in atmospheric studies, especially in satellite missions;
- ULB (Brussels, Belgium), which has provided the FT spectrometer and its know-how in spectroscopic analysis;

- and, GSMA (Reims, France), which has conceived and built two long path multiple reflection cells of respectively 5 and 50 m.

All the measurements made by this group and presented in the present paper were specifically undertaken in view of their use in atmospheric studies. This implies to operate under temperature and pressure conditions close to the ones prevailing in the atmosphere. The consequences of this approach will also be described.

LINE PARAMETERS MEASUREMENTS

The advantages of the Fourier transform spectrometers are numerous [20] and explain why such instruments have been used in the laboratory as well as in the field to determine line parameters or monitor atmospheric pollutants. Until recently, these instruments were essentially operated in the IR region. However, their use has now been extended to the UV and visible regions. In these regions, the absorption features are generally large or even diffuse, the spectra are often congested and it is not possible to separate individual absorption lines, hence the absorption cross-section concept, which will be illustrated in the next section. However some molecules (O_2 or H_2O for example) have spectra, in which individual lines are still present and observable up to the UV. Classical FT spectroscopy can therefore be extended in these spectral regions to deliver line parameters, such as the line positions, the intensities, and the self and foreign gas broadening coefficients.

To illustrate this, we will focus our attention on the measurements of the H_2O line parameters from the NIR to the near UV.

In the infrared region below 4500 cm^{-1}, the water vapor spectrum has been thoroughly investigated and line parameters of generally good quality are available through the HITRAN [16,17] or GEISA [18] databases. In the near infrared, the line lists are quite extensive but it is believed that some parameters are not sufficiently accurate [21]. It is in the visible and near ultraviolet, where the absorption is weak as compared to the infrared, that the data are the most incomplete [21]. An accurate analysis of the absorption of water vapor in the visible spectral range is particularly important for the atmospheric radiative budget, as the attenuation of the solar radiation is at its maximum in this region. A good knowledge of the weak lines in the visible region is also required for the retrieval of other atmospheric gases, which absorb in the same spectral range, as for instance NO_2.

Several sets of water vapor line parameters are available for the visible and NIR regions. Some cover a large spectral interval and provide comprehensive sets of parameters. For example, spectra recorded at the National Solar Observatory (Kitt Peak, Arizona) using the McMath Fourier transform

spectrometer gave rise to a large data set covering the 8000-25250 cm^{-1} spectral range [22-26]. This set forms the basis of the HITRAN 96 database [16] for H_2O. However, the pressure and temperature dependences were not studied, so that only line positions and intensities are available. These spectra were recently re-analyzed and complemented by new measurements [27] to provide a new data set in the 9650-11400 cm^{-1} spectral interval, which appeared in the 2000 edition of the HITRAN database [17]. Recently, in response to an announcement of opportunity of the European Space Agency (ESA), a new water vapor line list covering the spectral range from 8500 to 15000 cm^{-1} has been published [28-30]. The authors combine their new experimental data with the existing HITRAN database and with results of model calculations in order to provide a more complete list, including weaker lines of the water vapor, which are not accessible through laboratory measurements [31]. Finally, *Coheur et al.* [32] presented a complete and coherent set of line parameters, including the N_2-pressure broadening coefficients and shifts, in the 13000 – 26000 cm^{-1} spectral range. The latter set has the advantage of being, on the one hand much more extensive than former databases, with a cross-section dynamic range of 10^5, and on the other hand, fully homogeneous for the entire region investigated. In addition to these large spectral interval studies, other measurements have been performed on more restricted spectral regions [33-40].

The line intensities reported in different databases are often compared by a line by line comparison. However this technique is subject to statistical noise and does not take into account the presence of blended lines, which have been differently interpreted. Some authors prefer to perform the comparison on a small sample of 'best measured' lines [27]. But this method will overlook the different behaviour of the instrument in measuring very intense or very weak lines and might therefore not be statistically representative of the whole set of measurements. For these reasons, integrated cross-sections have been chosen as the best comparison between the existing large data sets, i.e. HITRAN [17], *Schermaul et al.* [31], and *Coheur et al.* [32]. Intensities integrated over each polyad present between 13000 and 26000 cm^{-1} are given in Table 1. For each data set, the number of lines and the integrated cross-sections for each polyad from 4ν to 8ν are given. In the case of the data set of *Schermaul et al.* [31], experimental and theoretically calculated values have been distinguished. The integrated cross-section over the entire spectral range of [32] is about 5% larger than that obtained from the HITRAN data set. As most of the intensity originates from the 4ν polyad, this difference can be explained as resulting from the systematic deviations for the stronger lines, which are on the average 3% more intense in [32]. The weak lines measured in [32] contribute, through their large number, to a further increase of the total absorption. The integrated cross-section of [31] obtained when considering only their experimental lines, is 2% larger than the one of [32], despite their smaller number. The reason is again that the stronger lines of the 4ν polyad have individually a larger cross-section (about 6% on average). The myriad of weak lines obtained from the [31] calculations contributes to the total integrated cross-section by an additional 3%.

Table 1: Comparison of the number of H_2O lines (N) and the integrated cross-sections (σ in cm molecule^{-1}) of the 4ν to 8ν polyads given in the most recent databases

	[17]		[31]				[32]	
			Experiment[a]		Theory			
Polyad	**N**	**σ**	**N**	**σ**	**N**	**σ**	**N**	**σ**
4ν	2101	1.58×10^{-21}	910	1.70×10^{-21}	7304	5.86×10^{-23}	3189	1.68×10^{-21}
4ν+δ	695	1.27×10^{-22}	1110	1.31×10^{-22}	1842	5.48×10^{-24}	1641	1.26×10^{-22}
5ν	1027	1.83×10^{-22}	1585	1.91×10^{-22}	364	3.10×10^{-24}	2119	1.80×10^{-22}
5ν+δ	356	1.38×10^{-23}	546	1.55×10^{-23}	68	2.45×10^{-26}	776	1.43×10^{-23}
6ν	279	2.28×10^{-23}	349[b]	2.27×10^{-23}			888	2.60×10^{-23}
6ν+δ	80	1.40×10^{-24}					257	1.92×10^{-24}
7ν	72	3.50×10^{-24}					373	4.97×10^{-24}
7ν+δ							45	2.28×10^{-25}
8ν							65	8.63×10^{-25}
total	**4610**	**1.93×10^{-21}**	**4500**	**2.06×10^{-21}**	**9588**	**6.72×10^{-23}**	**9353**	**2.03×10^{-21}**

[a] Includes HITRAN values (2301 lines in total) and new measurements
[b] Restricted to wave numbers below 20000 cm^{-1}

The determination of the self- and pressure-broadenings, as well as their temperature dependence relies on the choice of the line profile adopted to represent the observed data. Most studies are based on the use of Voigt profiles [29, 32]. However, *Grossmann and Browell* [35,36] have shown that using more sophisticated models such as these of *Galatry* [41] or of *Rautian and Sobel'man* [42] resulted in a better description of the observed profiles.

Coheur et al. [32] analyzed in detail the line profiles of pure water vapor and of H_2O/N_2 mixtures. They found a mean value of γ_{self} = 0.44 cm^{-1}atm^{-1} having considered all their experimental measurements weighted with their associated statistical errors. However the value of the self-broadening coefficient was shown to vary with the polyad number, increasing slightly from the 4ν to the 8ν. This could be due in part to the fact that the bands observed at higher energy have a larger proportion of rotational levels of low J", which are generally characterized by larger values of the broadening parameter [34]. A mean value of 0.0896 cm^{-1}atm^{-1} was found for γ_{N2} at 291.3 K over the entire visible range investigated in [32]. No obvious evolution with the polyad number nor with J" was observed. Measurements of the line position shifts due to the presence of the N_2 buffer gas suggested that most of the lines are red-shifted with increasing N_2 pressure and that this shift increases almost linearly with the polyad number.

Values of the self-broadening coefficient obtained by [32] agree generally well with those given in HITRAN (within 1%), but discrepancies up to 10% are observed for the broadening coefficients due to foreign gas. Large disagreements exist with the measurements of the broadening parameters reported in [31]. These values appear to be larger than those of [17,32] for the 4ν polyad by about 10%, but smaller for the other polyads. The water vapor line widths in a narrow portion of the visible region have been studied thoroughly in [34,35]. Their values of the self- and N_2-broadening parameters for a series of lines having a cross-section larger than 10^{-25} cm molecule^{-1} agree very well (to better than 2% on average) with the [32] values.

Values of N_2 induced shifts are scarce in the literature. The only other study [35], which investigated pressure shifts, reports values of δ_{N2} for wave numbers lower than 14000 cm^{-1}. These authors also observed that the large majority of lines are shifted towards smaller wave numbers with increasing N_2 pressure.

Atmospheric implications

Chagas et al. [9] studied the impact of updates of spectroscopic data on the short-wave absorption by atmospheric water vapor. They compared results obtained using different data sets (HITRAN-96 [16], HITRAN-99 [43], and ESA [31]). The HITRAN-99 parameters caused a globally and annually average increase in short-wave absorption of 0.26 Wm^{-2} and these of [31] an increase of 0.64 Wm^{-2} compared to the absorption found with the HITRAN-96 parameters. A similar study [44] analysed the impact of the H_2O line parameters on the absorption of solar radiation, comparing the HITRAN 2000 [17] and ESA [31] databases to the HITRAN-92 database. They found that the use of the newer data sets respectively induced an increase of the globally and annually absorption of 3.4 Wm^{-2} and 3.8 Wm^{-2}. *Learner et al.* [8] estimated the missing weak lines of water vapor from a statistical point of view and calculated the absorption of solar radiation associated therewith. They found that the additional absorption of solar radiation amounted to 1.5 to 2.5 Wm^{-2} depending on the model chosen to extrapolate the missing lines.

A recent study [7] compared measured and modelled direct beam irradiance. They found discrepancies in the 12000 cm^{-1} region, which they associated to missing H_2O lines in the spectroscopic databases. *Maurellis et al.* [45] investigated the retrieval of terrestrial precipitable water columns from the GOME (Global Ozone Monitoring Experiment) data. Their analysis technique was found to be very sensitive to the details of the line structure within the absorption spectrum. They expected that new laboratory measurements leading to more accurate line parameters as well as to more weak lines will contribute greatly to the accuracy of their method.

Veihelmann et al. [46] and *Smith and Newnham* [47] have evaluated the reliability of the various databases through their use in real atmospheric spectra interpretation. They investigated respectively the 585-600 nm (17100-16000 cm^{-1}) and the 830-985 nm (12050-10150 cm^{-1}) spectral regions. They found that the residuals between observed and modelled direct solar radiation were linked to missing lines in the database and mismatches in line intensities. To further illustrate this point, we have performed simulations of the pure water vapor spectrum using the data sets of HITRAN [17] and of *Coheur et al.* [32] in a 1D high-resolution radiative model [48,49,99] in the solar regime. Figure 1 clearly shows the differences existing in both investigated data sets, and especially the relative importance of the weak lines that are mostly not present in HITRAN.

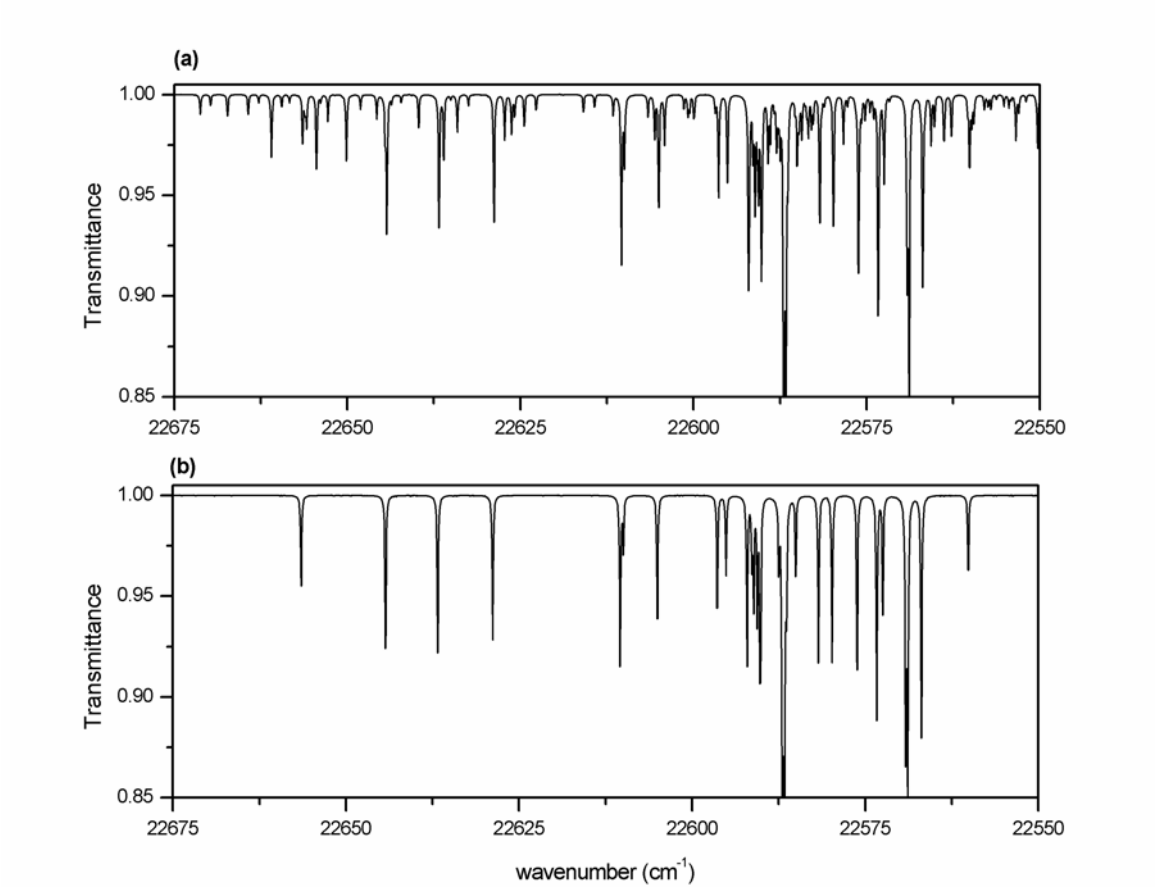

Figure 1: Simulations of a pure water vapor spectrum with (a) the line parameters obtained in [32] and (b) those listed in HITRAN [17].

All these examples illustrate the need for high quality spectroscopic line parameters for H_2O, and especially for measurement of weak lines.

UV-VISIBLE ABSORPTION CROSS-SECTIONS

UV-visible spectroscopy is now widely used to monitor several atmospheric species. This technique relies on the Beer-Lambert law, which describes the attenuation of light passing through an absorbing/diffusing medium. The following expression of the Beer-Lambert law is obtained when considering only one absorbing species characterized by its concentration n and its cross-section $\sigma(\lambda,T,P)$

$$I(\lambda) = I_0(\lambda)\exp\left[-nd\sigma(\lambda,T,P)\right] \quad (1)$$

where $I_0(\lambda)$ and $I(\lambda)$ are the incident and attenuated light intensities, and d is the length of the investigated path. The absorbance $A(\lambda)$ is defined as

$$A(\lambda) = \ln\left(\frac{I_0(\lambda)}{I(\lambda)}\right) = nd\sigma(\lambda,T,P) \quad (2)$$

Several remarks have to be made concerning expression (1): Firstly it has been derived for monochromatic light or infinite instrumental resolution. Secondly, the temperature (T) and pressure (P) dependences of the molecule cross-section appear explicitly. These two remarks have some implications on the use of the Beer-Lambert law when performing laboratory, as well as atmospheric measurements. They will be developed in more detail in the following paragraphs.

Polychromatic light and finite resolution

Equation (1) is only valid for monochromatic light. Expressed otherwise, this means that the cross-section present in this equation should have been measured with an infinitely small resolution, the instrumental function being represented by a Dirac function. When using the Beer-Lambert law with a finite resolution, as with real instruments, the above expression is only valid if the cross-section can be considered constant on the $[\lambda-\Delta\lambda,\lambda+\Delta\lambda]$ interval, where $\Delta\lambda$ is related to the resolution. If not, non-linear effects will be introduced. This is of great importance when recording spectra presenting sharp absorption features. Such spectra should be recorded at a resolution better than the width of the absorption structures present.

The effects of the non-linearities have been discussed in detail in [50]. When the resolution is equal or lower than the width of the observed feature, the absorbance is always proportional to the concentration of the absorber. When the resolution is larger than the line width, the measured absorbance decreases and remains constant at high concentrations. The larger the resolution, the larger the effect. The relation between the absorbance and the concentration is no longer linear. The

absorbance will be over-estimated at low concentrations, and under-estimated at high concentrations. Hanst and Hanst [50] concluded their analysis by stating a list of considerations to be observed when conducting quantitative analysis of gases. Some of them are worth citing here:

> "The absorption law is more likely to fail for small molecules that have individual spectral lines, because it is probable that the resolution bandwidth will be larger than the spectral line width"

> "As the resolution is increased, the absorbance errors are decreased"

> "When lines are not fully resolved, it is advantageous to record (…) the spectrum with small maximum absorbances"

These remarks are of great importance in laboratory measurements, but also in atmospheric studies. What has just been demonstrated is in contradiction with the common belief that cross-sections used in atmospheric studies should be obtained with the same instrument as the one used for recording the atmospheric spectra. Great care has also to be taken when convolving literature data, which is mandatory when laboratory and field spectra have not been recorded at the same resolution. The common practice is to convolve the cross-sections by the instrumental function. However, this can introduce errors which can impair on the precision of the retrieved concentrations. A direct convolution of the cross-sections supposes that the logarithmic function appearing in Expression (2) and the convolution function commute, i.e. these two operations can be applied in any order. This is, of course, not the case. This procedure leads to an absorbance scale, which is not linear with concentration. The solution is to use a synthetic spectrum $I(\lambda)$ calculated at high resolution from precise cross-sections and to convolute it to the desired resolution [51].

Temperature and pressure dependence of the cross-sections

Large temperature effects are expected and observed. They are due to the changes in the thermal populations of the vibrational and rotational levels, as the temperature changes. Since several studies [52-54] have pointed out the importance of this effect in atmospheric studies, it is now common practice to use absorption cross-sections measured at temperatures representative of the atmosphere being investigated.

On the contrary, pressure effects have only been investigated recently [55-58], and to our knowledge have not yet been implemented in atmospheric retrieval procedures in the UV-visible region.

As both effects are important in atmospheric studies, references obtained in the laboratory should be measured under temperature and pressure conditions as close as possible to atmospheric ones. This means operating at very low pressures of the molecule under investigation and with a buffer gas at pressures up to 1 atm. The low pressures imply the use of very long absorption paths to ensure a good accuracy on the cross-sections. Such long paths are generally obtained through the use of multiple reflection cells.

The importance of the temperature and pressure dependence will be illustrated with the NO_2 molecule, which has been investigated in several recent studies [54-70]. Except for the studies of *Bass et al.* [59] and *Leroy et al.* [62], they all agree in the description of the temperature effect: The absorption increases at the peak maxima and decreases at the peak minima when the temperature decreases. However, as shown by *Orphal* [70], the amplitude of the changes induced by the temperature differs greatly from one study to the other. In particular, the envelope of the NO_2 cross-section seems to be affected differently. *Orphal* [70] suggested that most of those discrepancies could be related to important baseline errors in several data sets. In most of the quoted studies, a linear dependence with temperature was observed or assumed. *Kirmse and Jost* [67] gave a more complex relation by separating the variation of the bell-shaped envelope and the superimposed spectral structures.

In a recent work [58], *Vandaele et al.* derived temperature dependent coefficients of the NO_2 absorption cross-section using all literature data obtained at a resolution better than 2 cm^{-1} and over a large wave number range. These authors considered 53 literature sets of data, covering the temperature range from 217 to 298.5 K in order to determine the temperature dependence in the 13200-42000 cm^{-1} spectral interval.

The evolution of the linear temperature coefficient in the 25000-33000 cm^{-1} spectral region has been explained [63,67] as resulting from the displacement and broadening of the bell curve of the cross-sections. The envelope of the absorption cross sections generated by vibrationally excited NO_2 molecules is larger than that of NO_2 in the ground state and is displaced towards the lower wave numbers. As the temperature increases, the relative intensities of the hot and cold bands are modified, and the bell shape is broadened and displaced. *Liévin et al.* [69] have calculated the absorption cross-sections using the reflection method applied to *ab initio* data. They could derive the envelope of the photoabsorption cross-sections of NO_2 by considering the two electronic transitions originating from the ground state $\tilde{X}^2A_1$ to the excited states $\tilde{A}^2B_2$ and $\tilde{B}^2B_1$. They also took into account the fact that the transitions could originate from the |010> vibrational level of $\tilde{X}^2A_1$. From their calculations at 220 and 300 K, we derived a linear temperature coefficient α ($\alpha = (\sigma_{220K} - \sigma_{300K})/(220 - 300)$). It is compared in Figure 2 to its corresponding value obtained from cross-sections calculated using a linear

regression [58]. These cross-sections were smoothed to eliminate all the fine structures, which are not reproduced by theory. The theoretical curve has been shifted by 600 cm^{-1}, as it is proposed in [69] in order to take into account a systematic error introduced by the reflection method itself. The *ab initio* curve does explain some of the features of the α curve, such as the two bumps and their relative position. However, it does not reproduce the relative amplitude observed for the two large structures. A residual N_2O_4 contribution cannot therefore be ruled out, as the structure observed at 30000 cm^{-1} corresponds to the main feature of the N_2O_4 absorption cross-sections.

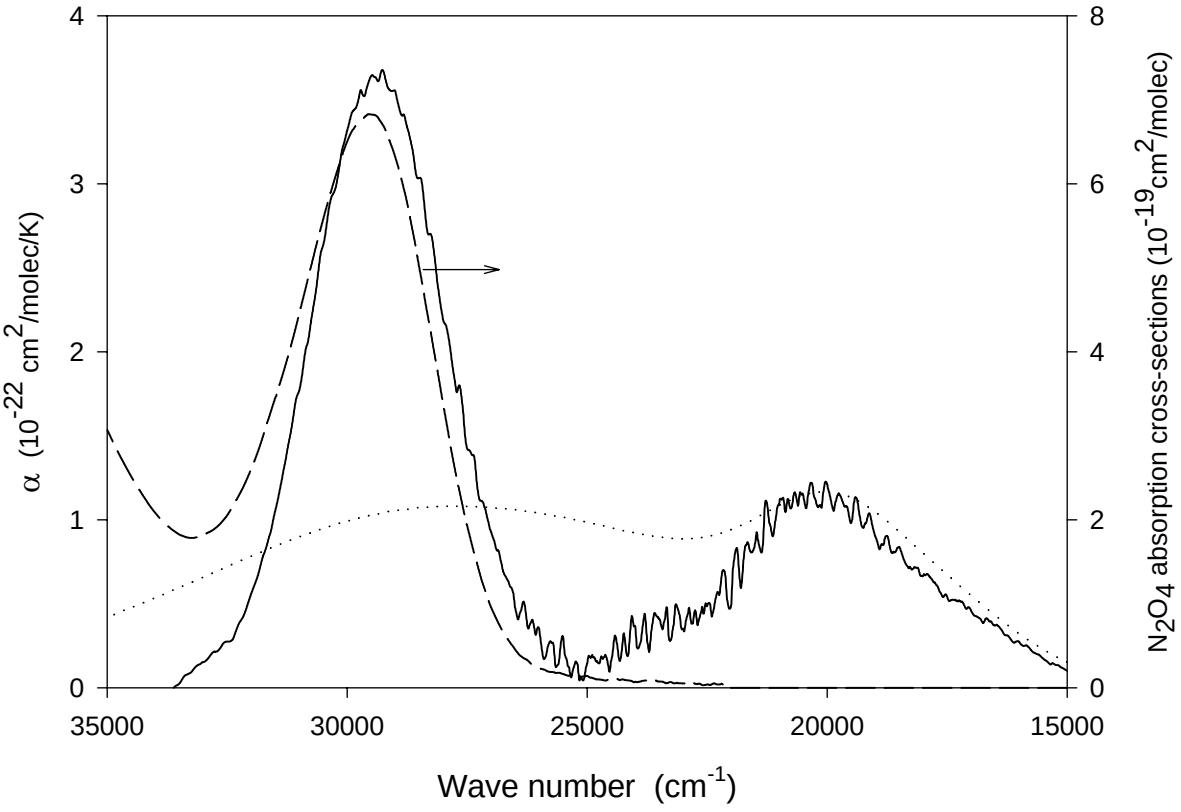

Figure 2: Temperature coefficient α calculated from the NO_2 absorption cross-sections at 220 and 300 K (—) using cross sections calculated with the linear regression of [58], (…) using cross sections obtained by the reflection method applied on *ab initio* data [69]. The absorption cross-sections of N_2O_4 [54] are also shown (- -).

Few studies have investigated the pressure effect on the NO_2 absorption cross-section. A pressure effect in pure NO_2 was observed in [54]. It might however be attributed to an experimental artefact, as

the resolution used in this work was not sufficient to fully resolve the NO_2 structures and as the absorption was strong. Both phenomena lead to deviations from the Beer-Lambert law and introduce non-linearities in the determinations of the cross-sections, as already explained. *Harder et al.* [55] mentioned measurements performed at high resolution (0.028 cm^{-1}) using a fixed number of NO_2 molecules, and increasing N_2 pressures. These measurements were complementary to high-resolution visible measurements of IO in the atmosphere [68]. A large variation (30 to 40%) in the differential amplitude with changing pressure was observed. These authors concluded however that the pressure effects are much larger than the temperature ones, which only become important at high spectral resolution. *Voigt et al.* [56] used mixtures of NO_2 and N_2 with total pressures of 100 and 1000 hPa. With only two total pressures, no systematic study of the pressure effect could be carried out. However, by convolving their low-pressure spectra with a Lorentzian function to reproduce their higher pressure data, these authors deduced a pressure broadening coefficient for the UV-visible part of the NO_2 spectrum. Their absolute value of the N_2 pressure broadening coefficient at 293 K is larger than those found in the mid- and near-IR, they attributed this difference to their low resolution, which was not sufficient to fully resolve the NO_2 structures.

Important pressure effects have been observed in spectra obtained with NO_2/air mixtures in [57]. These effects are enhanced at lower temperatures: For example, the decrease of the absorption cross-section for mixtures at the total pressure of 1013.2 hPa compared to pure NO_2 samples reached 50% at 294 K and 150% at 220 K. Using all literature spectra of mixtures of NO_2 in air or N_2, *Vandaele et al.* [58] analysed in detail the total pressure effect on the NO_2 absorption cross-section in the UV-visible region. By convolving pure NO_2 spectra with a Lorentzian function representing the pressure broadening effect and comparing the resulting spectra with spectra of mixtures of NO_2 in air or N_2, at different temperatures, these authors derived values of the pressure broadening coefficients and their temperature dependence. Values of $\gamma^0_{air}(T_0 = 296K)$ and $\gamma^0_{N2}(T_0 = 296K)$ have been found to be respectively 0.081(1) and 0.069(3) $cm^{-1}atm^{-1}$. The temperature dependence coefficient was found to be 0.8(1). This value is lower than most of the literature data, which propose values between 0.968(31) [61] and 1.02(4) [56]. Values of the pressure broadening coefficients are more commonly deduced in the IR and NIR regions, through the analysis of the profile of well-defined absorption lines [60,61,64-66]. Individual values of these coefficients vary considerably from line to line. For example *Dana et al.* [65] report values of γ^0_{air} ranging from 0.056 to 0.085 $cm^{-1}atm^{-1}$. Mean values of γ^0_{N2} deduced from IR and NIR spectra vary between 0.066 $cm^{-1}atm^{-1}$ [60] and 0.0723 $cm^{-1}atm^{-1}$ [65].

Atmospheric implications

Temperature and pressure effects on the absorption cross-section should be taken into account when retrieving amounts of atmospheric species from field spectra. This is most important for instruments probing different layers of the atmosphere, where temperature and pressure conditions may vary

considerably. Such instruments are for example, ground-based zenith sky and solar spectrometers and instruments on board satellites.

Sanders [52] analyzed in detail the influence of the NO_2 temperature dependence on the retrieval of stratospheric NO_2 from ground-based spectra. His interest stemmed from the observation that room temperature NO_2 cross-sections left persistent features in the residuals. He showed that using several cross-sections at different temperatures reduced these residuals by 50%. He also demonstrated that, while the use of one single cross-section at a well-chosen temperature reduced most of the residuals, the use of the information at different temperatures led to further improvement, particularly when tropospheric pollution was present. From his analysis, the optimal cross-section, when used alone, corresponded to a temperature of –29°C, which is found at an altitude of roughly 30 km, where the bulk of the NO_2 resides. As also shown in [71], using such a cross-section leads to a reduction of the NO_2 amount by about 15%.

As the pressure effect is only observable at high-resolution, it has not yet been implemented in atmospheric studies, in which the resolution is often lower, of the order of 0.2 to 1.0 nm. However, when instruments such as FT spectrometers are used at higher resolution, the pressure effect should be taken into account. *Wennberg et al.* [68] mentioned the possibility of separating the stratospheric and tropospheric NO_2 contributions based on the NO_2 pressure dependence.

COLLISION INDUCED SPECTRA

In the NIR and UV-visible regions, the main absorption of the solar radiation in the Earth's atmosphere is due to water vapor and oxygen. Oxygen presents absorption structures on the whole interval (see Figure 3), which correspond to different types of transitions:

- Strong absorption lines associated to the Herzberg I $\left(A^3\Sigma_u^+ - X^3\Sigma_g^-\right)$, Herzberg II $\left(c^1\Sigma_u^+ - X^3\Sigma_g^-\right)$, and Herberg III $\left(A'^3\Delta_u - X^3\Sigma_g^-\right)$ systems (41260-34480 cm^{-1});
- A true continuum that represents bound free transitions of O_2 from the ground state to the $O(^3P)+O(^3P)$ first dissociation limit (50000-41260 cm^{-1});
- Some diffuse bands underlying the Herzberg bands and showing a triplet structure and named after Wulf who first observed these in 1928 [72];
- O_2 IR and red atmospheric bands corresponding to transition from the ground state to respectively the $^1\Delta_g$ and $^1\Sigma_g^+$ excited electronic states;
- Diffuse bands from 7500 to 30000 cm^{-1}, some of which underly the O_2 IR and red structures.

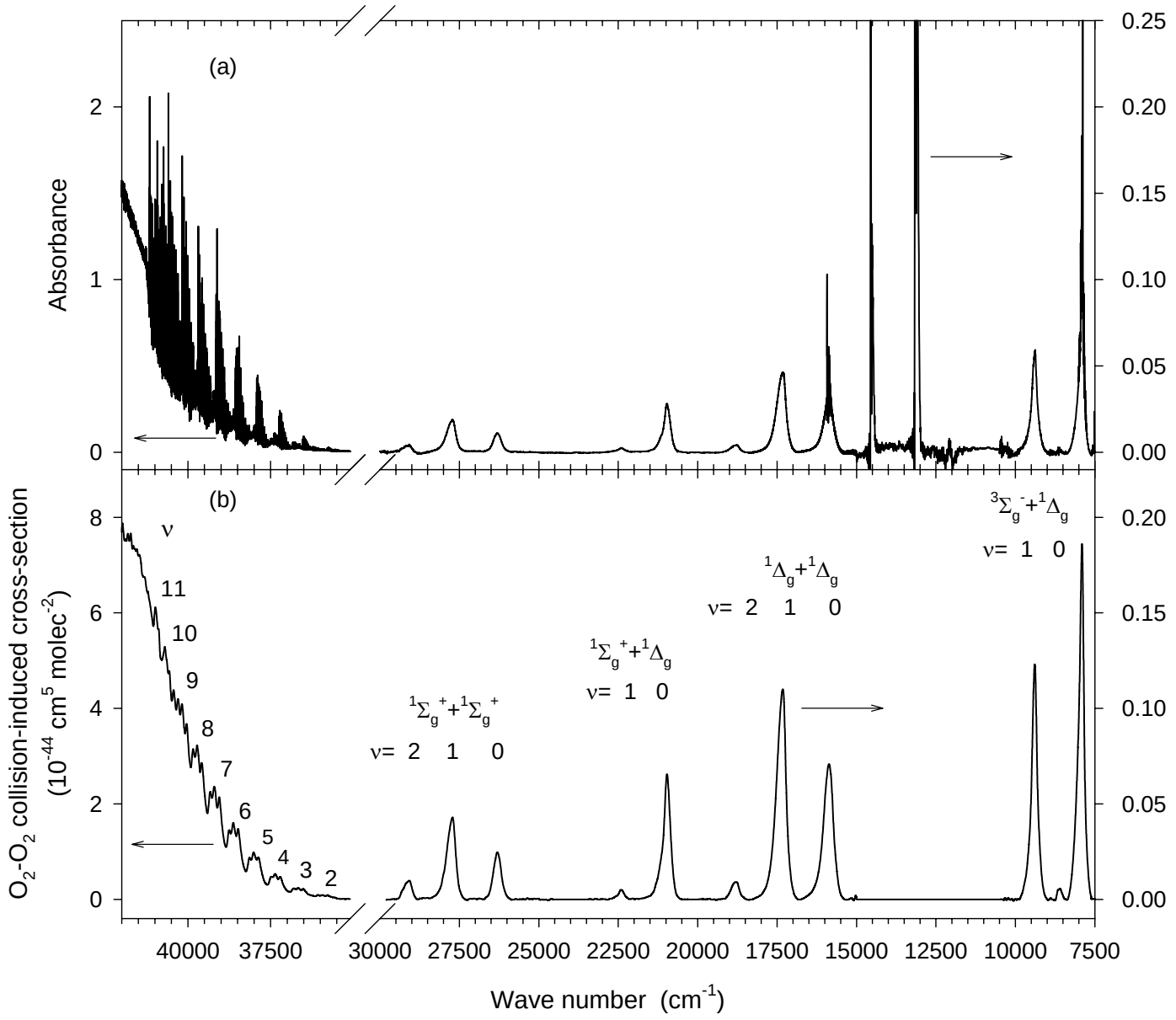

Figure 3: Oxygen absorption (a) and the O_2-O_2 collision-induced absorption cross-section (b) at room temperature from the UV to the NIR. Assigments and vibrational levels are also shown.

In the following chapter, we will particularly be interested in the diffuse bands, which are present in the O_2 absorption spectrum. These transitions have been investigated by several authors. The origin of these bands is still controversial. They are attributed either to the O_4 dimer, to a $(O_2)_2$ quasi-stable

complex or to collision-induced absorption (see [73] for a detailed description). A dimer such as O_4 can be described as a van der Waals molecule if it is bound only by weak intermolecular forces. At room temperature, the observation of dimers is not expected as the average kinetic energy is much greater than the weak attraction. In a quasi-stable or metastable complex, a common binding molecular orbital may exist during the collision [74, 75]. *Long and Ewing* [76] found that the absorption in the visible and the NIR bands is broad and featureless, indicating its origin in an unbound collision complex. Several other studies [77-80] have led to the interpretation of these bands as collision-induced electronic transitions, with no evidence for the existence of quasi-stable complexes. The spectroscopy of the collision complex of O_2 is in fact poorly understood. The detailed mechanism for the induced absorption is still unknown. The strengths of the 1.06 μm and 1.27 μm bands (9390 and 7900 cm^{-1}), which correspond to the ${}^1\Delta_g - {}^3\Sigma_g^-$ transition with ν=1 and 0 respectively, are roughly the same, whereas the ν=2 and subsequent transitions are far weaker [81]. More surprisingly, the red system $\left({}^1\Sigma_g^+ - {}^3\Sigma_g^-\right)$ displays virtually no O_2-O_2 component. *Cho et al.* [77] report a factor of 10 in the intensity in the red region compared to the NIR system. Due to their experimental conditions, nor *Greenblatt et al.* [82] nor *Hermans et al.* [83,84] could find any O_2-O_2 contribution in the red system. In the UV region, O_2 absorption displays some broad absorption that is pressure-dependent. It has been attributed to collision dimers [85,86] and more recently to collision-induced absorption [87].

We will further describe results obtained by our group. These are based on a series of spectra obtained with a FT spectrometer coupled to 2 multiple reflection cells of respectively 5 and 50 m base length (see [83,87] for a detailed description of the experimental conditions). Absorption paths of 60 m to 1002 m were used; measurements of pure O_2 and of O_2-N_2 and O_2-Ar mixtures were performed at different pressures. Spectra at 0.02, 0.12, and 2 cm^{-1} were recorded from the NIR to the UV. The high-resolution spectra allowed the measurements and the analysis of the Herzberg systems [88-90]. The rotational assignments of these bands have been extended in the most intense bands, hereby allowing the derivation of more accurate molecular constants. New vibrational levels were observed near the dissociation limit. The new parameters of the Herzberg bands were used to isolate the contribution of the underlying continuum and diffuse bands [87, 83]. The high-resolution spectra also provided the line parameters of the ${}^1\Delta_g(\nu=0) - {}^3\Sigma_g^-$ and ${}^1\Sigma_g^+(\nu=2) - {}^3\Sigma_g^-$ bands, allowing the extraction of the contribution of the diffuse feature in the NIR and visible regions.

The absorbance (A) shown in Figure 3(a) is related to the oxygen pressure through the following expression

$$A = (\sigma_{O2} + \sigma_{O2C}) P_{O2}\, d\, k + (\sigma_{O2-O2} + \gamma\, \sigma_{O2-X}) P_{O2}^2\, d\, k^2 + A_{RS} \qquad (3)$$

where σ_{O2} and σ_{O2C} are the O_2 band systems and continuum absorption cross-sections (cm^2 $molecule^{-1}$), $\sigma_{O2\text{-}O2}$ and $\sigma_{02\text{-}X}$ are the collision induced absorption cross-sections (cm^5 $molecule^{-2}$), d is the path length (cm), P_{O2} is the oxygen pressure (hPa), γ is the X/O_2 mixing ratio, A_{RS} is the absorbance equivalent to the photon loss due to Rayleigh scattering, and k is equal to N_0T_0/P_0T where N_0 is the Loschmidt number, T_0 and P_0 are the normal temperature and pressure (K and hPa). For pure O_2 experiments, γ equals zero. The total pressure of the O_2/X mixtures experiments was varied, but the value of γ was maintained constant and close to the atmospheric N_2/O_2 ratio (≈4).

On the right-hand side of Equation (3), the first term varies linearly with pressure and includes the absorption of the O_2 bands systems (Herzberg systems, IR and red atmospheric discrete bands) and the Herzberg continuum. The second term corresponds to the quadratic pressure-dependent part of the absorbance and is due to O_2-O_2 and O_2-X collision-induced absorptions (CIA). Measurements performed at various pressures from 100 to 1000 hPa allow to separate all the components of the oxygen spectrum. In the NIR and visible regions (Figure 3(a)), two types of absorption features are observed: Structured absorption associated with the monomer transitions $\left({}^1\Delta_g - {}^3\Sigma_g^- \text{ and } {}^1\Sigma_g^+ - {}^3\Sigma_g^-\right)$ and diffuse bands attributed to O_2-O_2 transitions. These band systems are due to transitions between the three lowest electronic states of O_2 and involve the excitation of one molecule:

$$\begin{aligned} {}^1\Delta_g + {}^3\Sigma_g^- &\leftarrow {}^3\Sigma_g^- + {}^3\Sigma_g^- \\ {}^1\Sigma_g^+ + {}^3\Sigma_g^- &\leftarrow {}^3\Sigma_g^- + {}^3\Sigma_g^- \end{aligned} \tag{4}$$

or of two molecules:

$$\begin{aligned} {}^1\Delta_g + {}^1\Delta_g &\leftarrow {}^3\Sigma_g^- + {}^3\Sigma_g^- \\ {}^1\Delta_g + {}^1\Sigma_g^+ &\leftarrow {}^3\Sigma_g^- + {}^3\Sigma_g^- \\ {}^1\Sigma_g^+ + {}^1\Sigma_g^+ &\leftarrow {}^3\Sigma_g^- + {}^3\Sigma_g^- \end{aligned} \tag{5}$$

The O_2-O_2 CIA cross-section at room temperature is presented in Figure 3(b) from 42000 to 7500 cm^{-1}. The 35000-30000 cm^{-1} region is omitted from the Figure because the absorption goes to zero. The assignments of the O_2-O_2 collision-induced bands are also shown in this Figure. From the detailed analysis of the position of the triplets diffuse bands underlying the Herzberg bands [87], strong similarities were found with the ${A'}^3\Delta_u - X^3\Sigma_g^-$ transition. This reinforces the argument that the Wulf bands are due to an enhancement of this forbidden transition caused by the relaxation of the dipole-forbidden selection rule during collision.

Visible and NIR peak absorption of the O_2-O_2 cross-section are given in Table 2 and are compared with values of the literature. Values from [84] are in good agreement with those of [82] and [91] given the high uncertainties on those measurements. It should be noted that the results from [92] and [93] have been obtained from atmospheric spectra.

Table 2: O_2-O_2 peak collision-induced absorption cross-section (x 10^{46} cm^5 $molecule^{-2}$)

Wavenumber (cm^{-1})	Peak collision-induced absorption cross-section (10^{-46} cm^5 $molecule^{-2}$)					
	[82] 296 K	[84] 293 K	[91] 290 K	[92] 296 K	[93] 278 K	[100] 283 K
29150	1.2(1)	1.0	-	-	0.70(24)	-
27760	4.1(4)	4.3	4.4	-	5.4(15)	-
26320	2.4(2)	2.5	2.2	-	<1.4	-
22420	0.57(6)	0.6	0.7	-	1.0(12)	-
20970	6.3(6)	6.6	5.5	6.49(3)	5.9(18)	8.34(83)
18810	1.0(1)	1.1	1.5	1.1(2)	-	1.23(38)
17360	11.0(1)	11.1	9.8	11.1(4)	16.0(6)	11.75(20)
15870	7.2(7)	7.1	6.9	-	-	7.9(15)
9390	12.0(1)	12.6	12.0	-	-	-
7900	-	18.6	-	-	-	-

As the two diffuse bands in the NIR range involve the excitation of a single oxygen molecule, these transitions can also be induced by a foreign gas. Measurements of the O_2-N_2 CIA cross-sections have been reported in the literature [84,94,95] but they greatly disagree on the amplitude of the effect of the buffer gas. In [84], the amplitude of the O_2-N_2 cross-section at 7900 cm^{-1} (1.27 μm) is 2.3 times smaller than the corresponding O_2-O_2 amplitude. Similarly, *Maté et al.* [94] found a factor of 2.38. No O_2-N_2 contribution to the absorption at 9390 cm^{-1} (1.06 μm) is observed in [84].

In the UV, $\sigma_{02\text{-}X}$ (with X=N_2 or Ar) were also obtained [87]. It was demonstrated that the intensity of the Wulf bands depended on the total pressure, and that the shape and position of the triplets were independent of the nature of the foreign gas. In other words, the Wulf bands exhibit the same feature whatever the collision partner. This observation provides evidence that the Wulf bands are produced by collision-induced absorption, and not from dimer absorption. In agreement with previous studies [86, 96, 97], O_2-N_2 and O_2-Ar CIA cross-sections were found to be almost equal, and

approximatively twice smaller than the O_2-O_2 CIA cross-section. However the differences between O_2-O_2 and O_2-X cross-sections recorded at the same total pressure suggest the presence of an additional unknown mechanism involving only O_2-O_2 interactions.

Atmospheric implications

Techniques such as DOAS (Differential Optical Absorption Spectroscopy) or DIAL (Differential Absorption LIDAR) require the knowledge of the absorption cross-sections of all the absorbers present in the investigated spectral region. Although the retrieval of O_2 and O_2-O_2 or O_2-X may not be of interest in itself, their absorption structures must be accounted for in the retrieval of the other trace gases. A comparison between two datasets of O_2-O_2 absorption cross-sections has been made through retrievals of NO_2, O_3, BrO, and OClO in the visible region [84]. The differences in the slant columns varied from 2 to 6% depending on the molecule. The quality of the fit, inferred from the RMS values of the residuals, also varied from one dataset to the other, and from molecule to molecule. The best fit was obtained for O_3 and NO_2 when using *Greenblatt*'s data [82]. On the contrary, a better fit is obtained for OClO when using the [83] data, and BrO is not sensitive to the choice of the CIA cross-section.

It has been suggested [98] that the IR diffuse bands (at 1.06, 1.27, and 1.58 μm) may be responsible in part for the discrepancy between modelled and observed atmospheric short-wave absorption. However, *Mlawer et al.* [99] indicate that their contribution reached approximatively 0.42 Wm^{-2} to the globally averaged solar absorption, which is significantly less than the observed discrepancy between measurements and models. When combined with O_2 absorption in the visible and near-UV, a globally average clear-sky absorption of 0.53 to 1.22 Wm^{-2} is obtained [13, 14, 99]. *Zender* [15] characterized the spatial and temporal distributions of the O_2-X forcing, showing that it displays stronger gradients compared to the monomer forcing, which can be explained mostly by the quadratic dependence of the O_2-N_2 abundance on the O_2 and N_2 abundances. This causes for example a 20% increase of the O_2-N_2 abundance in the Arctic relative to the Tropics. They found that the globally average O_2-X annual mean absorption lies between 0.75 and 1.2 Wm^{-2}, the range of values representing the uncertainties, which are essentially due to uncertainties on the O_2-X absorption cross-section. Although small compared to the actual missing absorption (about 30 Wm^{-2}), absorption of O_2-O_2 and O_2-X should still be included in radiation models.

Pfeilsticker et al. [13] and *Solomon et al.* [14] found a small increase of the globally average absorption of O_2-X when considering all-sky conditions instead of clear-sky conditions (0.57 Wm^{-2} instead of 0.53 Wm^{-2}; 0.96-1.32 Wm^{-2} instead of 0.87-1.22 Wm^{-2} respectively). *Zender* [15] on the contrary found no significant difference. This makes it clear that complexes cannot solve the solar absorption discrepancies associated with clouds.

CONCLUSIONS

High-resolution UV-visible-NIR spectroscopy is now a widely used technique for laboratory studies as well as for field measurements. Recent developments in atmospheric soundings from satellites and ground-based instruments, have stimulated new measurements in the laboratory. High-accuracy data are needed. Moreover, temperature and pressure effects should also be determined with high precision. In this review, we have stressed the importance of obtaining data in the laboratory under conditions similar to the ones prevailing in the atmosphere. This is important for the temperature dependence, but also for the pressure broadening effect. In the case of NO_2, taking these dependences into account can lead to up to 15% differences in the retrieved abundances. Moreover, as the shapes of the structures are modified by temperature, residuals depend heavily on the chosen temperature. We would like to emphasize once more the crucial role played by the spectral resolution of the measurements. If the latter is not good enough to resolve all the structures present in the spectrum, non-linearities are introduced, which may impact on the retrieved abundances.

The examples discussed in this work have been chosen such as to cover the entire spectral range from the NIR to the UV, and to be representative of different types of data that can be acquired through spectroscopy. The line parameters, including their position, intensity, self and pressure broadening coefficients, need to be determined with high accuracy for their use in atmospheric retrieval or atmospheric radiative transfer modelling. Neither missing O_2-O_2 or O_2-N_2, errors on H_2O line intensities, nor H_2O missing lines can resolve the discrepancies existing between observed and modelled Earth's atmosphere absorption. Their individual contributions are indeed too small and seem even negligible. Nevertheless they must be taken into account in modelling studies.

Accurate knowledge of the absorption cross-sections of H_2O, and O_2, and its complexes O_2-O_2 and O_2-N_2, is needed for the removal of their structures from atmospheric spectra allowing the accurate determination of the other absorbing species.

We have shown that despite the growing complexity of the techniques implemented in the laboratory, high quality data are still needed for atmospheric studies. In the future, emphasis should be put on the development of techniques with improved sensitivity in order to measure even weaker absorptions. On the other hand, instruments such as Fourier transform spectrometers offer the possibility to cover a large spectral range, and possess an internal wave number calibration. Those advantages should also be exploited.

ACKNOWLEDGMENTS

This research was supported by the Belgian State-Prime Minister's Service- Federal Offices for Scientific, Technical and Cultural Affairs and the Fonds National de la Recherche Scientifique (Belgium). We are grateful for the support provided by the Centre National de Recherche Scientifique (France) and the Institut National des Sciences de l'Univers (France) through the Programme National de Chimie Atmosphérique.

REFERENCES

1. Cess, R.D. 1995, Science 267, 496
2. Pilewskie, P. and Valero, F.P.J. 1995, Science 267, 1626
3. Kato, S., Ackerman, T.P., Clothiaux, E.E., Mather, J.H., Mace, G.G., Wesely, M.L., Murcray, F. and Michalsky, J.J. 1997, J. Geophys. Res. 102, 25881
4. Halthore, R.N., Nemesure, S., Schwartz, S.E., Imre, D.G., Berk, A., Dutton, E.G. and Bergin, M.H. 1998, Geophys. Res. Lett. 25, 3591
5. Halthore, R.N. and Schwartz, S.E. 2000, J. Geophys. Res. 105, 20165
6. Fu, Q., Lessings, G., Higgins, J., Charlock, T.P., Chylek, P. and Michalsky, J.J. 1998, Geophys. Res. Lett. 25, 1169
7. Mlawer, E.J., Brown, P.P., Clough, S.A., Harrison, L.C., Michalsky, J.J. and Shippert, T. 2000, Geophys. Res. Lett. 27, 2653
8. Learner, R.C.M., Zhong, W., Haigh, J.D., Belmiloud, D. and Clarke, J. 1999, Geophys. Res. Lett. 26, 3609
9. Chagas, J.C.S., Newnham, D.A., Smith, K.M. and Shine, K.P. 2001, Geophys. Res. Lett. 28, 2401
10. Arking, A. 1996, Science 273, 779
11. Chylek, P. and Geldart, D.J. 1997, Geophys. Res. Lett. 24, 2015
12. Headrick, J.E. and Vaida, V. 2001, Phys.Chem. Earth (C) 26, 479
13. Pfeilsticker, K., Erle, F. and Platt, U. 1997, J. Atmos. Sciences 54, 933
14. Solomon, S., Portmann, R.W., Sanders, R.W. and Daniel, J.S. 1998, J. Geophys. Res. 103, 3847
15. Zender, C.S. 1999, J. Geophys. Res. 104, 24471
16. Rothman, L.S., Rinsland, C.P., Goldman, A., Massie, S.T., Edwards, D.P., Flaud, J.-M., Perrin, A., Camy-Peyret, C., Dana, V., Mandin, J.-Y., Schroeder, J., McCann, A., Gamache, R.B., Wattson, R.B., Yoshino, K., Chance, K.V., Jucks, K.W., Brown, L.R., Nemtchinov, V. and Varanasi, P. 1998, J. Quant. Spectrosc. Radiat. Transfer 60, 665
17. Rothman, L.S., Barbe, A., Benner, C., Brown, L.R., Camy-Peyret, C., Carleer, M., Chance, K.V., Clerbaux, C., Dana, V., Devi, M., Fayt, A., Flaud, J.-M., Gamache, R.B., Goldman, A.,

Jaquemart, D., Jucks, K.W., Lafferty, W., Mandin, J.-Y., Massie, S.T. and Newnham, D.A. in preparation, J. Quant. Spectrosc. Radiat. Transfer

18. Jaquinet-Husson, N., Arié, E., Ballard, J., Barbe, A., Bjoraker, G., Bonnet, B., Brown, L.R., Camy-Peyret, C., Champion, J.-P., Chédin, A., Chursin, A., Clerbaux, C., Duxbury, G., Flaud, J.-M., Fourrié, N., Fayt, A., Granier, C., Gamache, R.B., Goldman, A. and Golovko, V. 1999, J. Quant. Spectrosc. Radiat. Transfer 61, 4205
19. Newnham, D.A. 2001, NERC Report
20. Griffiths, P.R. and de Haseth, J.A. 1986, Fourier Transform Infrared Spectrometry, John Wiley & Sons, pp 656
21. ESA contract No 13048/98/NL/GD
22. Camy-Peyret, C., Flaud, J.-M., Mandin, J.-Y., Chevillard, J.-P., Brault, J., Ramsay, D., Vervloet, M. and Chauville, J. 1985, J. Molec. Spectrosc. 113, 208
23. Mandin, J.-Y., Chevillard, J.-P., Camy-Peyret, C. and Flaud, J.-M. 1986, J. Molec. Spectrosc. 116, 167
24. Mandin, J.-Y., Chevillard, J.-P., Flaud, J.-M. and Camy-Peyret, C. 1988, Can. J. Phys. 66, 997
25. Chevillard, J.-P., Mandin, J.-Y., Flaud, J.-M. and Camy-Peyret, C. 1989, Can. J. Phys. 67, 1065
26. Toth, R.A. 1994, J. Molec. Spectrosc. 166, 176
27. Brown, L.R., Toth, R.A. and Dulick, M. 2002, J. Molec. Spectrosc. 212, 57
28. Belmiloud, D., Schermaul, R., Smith, K.M., Zobov, N.F., Brault, J.W., Learner, R.C.M., Newnham, D.A. and Tennyson, J. 2000, Geophys. Res. Lett. 27, 3703
29. Schermaul, R., Learner, R.C.M., Newnham, D.A., Williams, R.G., Ballard, J., Zobov, N.F., Belmiloud, D. and Tennyson, J. 2001, J. Molec. Spectrosc. 208, 32
30. Schermaul, R., Learner, R.C.M., Canas, A.A.D., Brault, J.W., Polyansky, O.L., Belmiloud, D., Zobov, N.F. and Tennyson, J. in preparation. J. Molec. Spectrosc.
31. Schermaul, R., Learner, R.C.M., Newnham, D.A., Ballard, J., Zobov, N.F., Belmiloud, D. and Tennyson, J. 2001, J. Molec. Spectrosc. 208, 43
32. Coheur, P.-F., Fally, S., Carleer, M., Clerbaux, C., Colin, R., Jenouvrier, A., Mérienne, M.-F., Hermans, C. and Vandaele, A.C. 2002, J. Quant. Spectrosc. Radiat. Transfer 74, 493
33. Wilkerson, T.D., Schwemmer, G., Gentry, B. and Giver, L.P. 1979, J. Quant. Spectrosc. Radiat. Transfer 22, 315
34. Grossmann, B. and Browell, E.V. 1989, J. Molec. Spectrosc. 136, 264
35. Grossmann, B. and Browell, E.V. 1989, J. Molec. Spectrosc. 138, 562
36. Grossmann, B. and Browell, E.V. 1991, J. Quant. Spectrosc. Radiat. Transfer 45, 339
37. Singh, K. and O'Brien, J.J. 1994, J. Molec. Spectrosc. 167, 99
38. Kalmar, B. and O'Brien, J.J. 1998, J. Molec. Spectrosc. 192, 386
39. Xie, J., Paldus, B.A., Wahl, E.H., Martin, J., Owano, T.G., Kruger, C.H., Harris, J.S. and AZare, R.N. 1998, Chemical Physics Letters 284, 387

40. Parvitte, B., Zéninari, V., Pouchet, I. and Durry, G. 2002, J. Quant. Spectrosc. Radiat. Transfer 75, 493
41. Galatry, L. 1961, Phys. Rev. 122, 1218
42. Rautian, S.G. and Sobel'man, I.I. 1967, Sov. Phys. Usp. 9, 701
43. Giver, L.P., Chackerian Jr., C. and Varanasi, P. 2000, J. Quant. Spectrosc. Radiat. Transfer 66, 101
44. Bennartz, R. and Lohmann, U. 2001, Geophys. Res. Lett. 28, 4591
45. Maurellis, A.N., Lang, R., van der Zande, W.J., Aben, I. and Ubachs, W. 2000, Geophys. Res. Lett. 27, 903
46. Veihelmann, B., Lang, R., Smith, K.M., Newnham, D.A. and van der Zande, W.J. in press, Geophys. Res. Lett.
47. Smith, K.M. and Newnham, D.A. 2001, Geophys. Res. Lett. 28, 3115
48. Clough, S.A., Iacono, M.J. and Moncet, J.-L. 1992, J. Geophys. Res. 97, 15761
49. Clough, S.A. and Iacono, M.J. 1995, J. Geophys. Res. 100, 16519
50. Hanst, P.L. and Hanst, S.T. 1994. In:Sigrist, M.W. (Editor), Gas measurement in the fundamental infrared region, 335, John Wiley & Sons, Inc.
51. Vandaele, A.C. and Carleer, M. 1999, Appl. Opt. 38, 2630
52. Sanders, R.W. 1996, J. Geophys. Res. 101, 20945
53. Richter, A., "Absorptionsspektroskopische Messungen Stratosphärischer Spurengase Über Bremen, 53°N", Ph.D. dissertation (Üniversität Bremen, Bremen, 1997).
54. Vandaele, A.C., Hermans, C., Simon, P.C., Carleer, M., Colin, R., Fally, S., Mérienne, M.-F., Jenouvrier, A. and Coquart, B. 1998, J. Quant. Spectrosc. Radiat. Transfer 59, 171
55. Harder, J.W., Brault, J.W., Johnston, P.V. and Mount, G.H. 1997, J. Geophys. Res. 102, 3861
56. Voigt, S., Orphal, J. and Burrows, J.P. 2002, J. Photochem. Photobiol. A 149, 1
57. Vandaele, A.C., Hermans, C., Fally, S., Carleer, M., Colin, R., Mérienne, M.-F., Jenouvrier, A. and Coquart, B. in press, J. Geophys. Res.
58. Vandaele, A.C., Hermans, C., Fally, S., Carleer, M., Mérienne, M.-F., Jenouvrier, A., Coquart, B. and Colin, R. in press, J. Quant. Spectrosc. Radiat. Transfer
59. Bass, A.M., Ledford, A.E., Jr. and Laufer, A.H. 1976, Journal of Research of the National Bureau of Standards, A : Physics and Chemistry 80A, 143
60. Malathy Devi, V., Fridovich, B., Jones, G.D., Snyder, D.G.S., Das, P.P., Flaud, J.M., Camy-Peyret, C. and Narahari Rao, K. 1982, J. Molec. Spectrosc. 93, 179
61. Malathy Devi, V., Fridovich, B., Jones, G.D., Snyder, D.G.S. and Neuendorffer, A. 1982, Appl. Opt. 21, 1537
62. Leroy, B., Rigaud, P. and Hicks, E. 1987, Annales Geophysicae 5A, 247
63. Davidson, J.A., Cantrell, C.A., McDaniel, A.H., Shetter, R.E., Madronich, S. and Calvert, J.G. 1988, J. Geophys. Res. 93, 7105

64. May, R.D. and Webster, C.R. 1990, Geophys. Res. Lett. 17, 2157
65. Dana, V., Mandin, J.-Y., Allout, M.-Y., Perrin, A., Régalia, L., Barnbe, A., Plateaux, J.-J. and Thomas, X. 1997, J. Quant. Spectrosc. Radiat. Transfer 57, 445
66. Gianfrani, L., Santovito, M.R. and Sasso, A. 1997, J. Molec. Spectrosc. 186, 207
67. Kirmse, B. and Jost, R. 1997, J. Geophys. Res. 102, 16089
68. Wennberg, P.O., Brault, J.W., Hanisco, T.F., Salawitch, R.J. and Mount, G.H. 1997, J. Geophys. Res. 102, 8887
69. Liévin, J., Delon, A. and Jost, R. 1998, J. Chem. Phys. 108, 8931
70. Orphal, J. 2002, ESA-Technical Note MO-TN-ESA-GO-0302, March 15
71. Vandaele, A.C., Hermans, C., Simon, P.C., Van Roozendael, M., Guilmot, J.M., Carleer, M. and Colin, R. 1996, J. Atm. Chem. 25, 289
72. Wulf, O.R. 1928, Proc. Nat. Acad. Sci. (US) 14, 609
73. Krupenie, P.H. 1972, J. Phys. Chem. Ref. Data 1,
74. Johnston, H.S., Paige, M. and Yao, F. 1984, J. Geophys. Res. 89, 11665
75. Blake, A.J. and McCoy, D.G. 1987, J. Quant. Spectrosc. Radiat. Transfer 38, 113
76. Long, C.A. and Ewing, G.E. 1973, J. Chem. Phys. 58, 4824
77. Cho, C.W., Allin, E.J. and Welsh, H.L. 1963, Can. J. Phys. 41, 1991
78. Blickensderfer, R.P. and Ewing, G.E. 1969, J. Chem. Phys. 51, 873
79. Blickensderfer, R.P. and Ewing, G.E. 1969, J. Chem. Phys. 51, 5284
80. Tabisz, G.C., Allin, E.J. and Welsh, H.L. 1969, Can. J. Phys. 47, 2859
81. Badger, R.M., Wright, A.C. and Witlock, R.F. 1965, J. Chem. Phys. 43, 4345
82. Greenblatt, G.D., Orlando, J.J., Burkholder, J.B. and Ravishankara, A.R. 1990, J. Geophys. Res. 95, 18577
83. Hermans, C., Vandaele, A.C., Coquart, B., Jenouvrier, A., Mérienne, M.-F., Fally, S., Carleer, M. and Colin, R. 2001, IRS 2000: Current Problems in Atmospheric Radiation, 639
84. Hermans, C., Vandaele, A.C., Fally, S., Carleer, M., Colin, R., Coquart, B., Jenouvrier, A. and Mérienne, M.-F. 2002, NATO Advanced Research Workshop, Weakly Interacting Molecular Pairs: Unconventional Absorbers of Radiation in the Atmosphere
85. Shardanand, R. 1969, Phys. Rev. 186, 5
86. Shardanand, R. 1977, J. Quant. Spectrosc. Radiat. Transfer 18, 525
87. Fally, S., Vandaele, A.C., Carleer, M., Hermans, C., Jenouvrier, A., Mérienne, M.-F., Coquart, B. and Colin, R. 2000, J. Molec. Spectrosc. 204, 10
88. Jenouvrier, A., Mérienne, M.-F., Coquart, B., Carleer, M., Fally, S., Vandaele, A.C., Hermans, C. and Colin, R. 1999, J. Molec. Spectrosc. 198, 136
89. Mérienne, M.-F., Jenouvrier, A., Coquart, B., Carleer, M., Fally, S., Colin, R., Vandaele, A.C. and Hermans, C. 2000, J. Molec. Spectrosc. 202, 171

90. Mérienne, M.-F., Jenouvrier, A., Coquart, B., Carleer, M., Fally, S., Colin, R., Vandaele, A.C. and Hermans, C. 2001, J. Molec. Spectrosc. 207, 120
91. Dianov-Klokov, V.I. 1964, Opt. Spectrosc. 16, 224
92. Osterkamp, H., Ferlemann, F., Harder, H., Perner, D., Platt, U., Schneider, M. and Pfeilsticker, K. 1997, Proc. of the 4th European Symposium on Polar Stratospheric Ozone, Schliersee, Germany, 22-26 September, 478
93. Perner, D. and Platt, U. 1980, Geophys. Res. Lett. 7, 1053
94. Maté, B., Lugez, C., Fraser, G.T. and Lafferty, W. 1999, J. Geophys. Res. 104, 30585
95. Smith, K.M. and Newnham, D.A. 2000, J. Geophys. Res. 105, 7383
96. Dianov-Klokov, V.I. 1966, Opt. Spektrosk. 21, 233
97. Shardanand, R. 1978, J. Quant. Spectrosc. Radiat. Transfer 20, 265
98. Murcray, F., Goldman, A., Landry, J.C. and Stephen, T.M. 1997, Geophys. Res. Lett. 24, 2315
99. Mlawer, E.J., Clough, S.A., Brown, P.D., Stephen, T.M., Landry, J.C., Goldman, A. and Murcray, F. 1998, J. Geophys. Res. 103, 3859
100. Newnham, D.A. and Ballard, J. 1998, J. Geophys. Res. 103, 28801